Evaluation of Dimension Stone According to Resistance to Freeze–Thaw Cycling to Use in Cold Regions

Reza Mikaeil[1] , **Akbar Esmaeilzade[2]** , **Sina Shaffiee Haghshenas[3]** , **Mohammad Ataei[4]** , **Sina Hajizadehigdir[5], Amir Jafarpour[6], Tae-Hyung Kim[7], Zong Woo Geem[8*]**

1. Associate Professor, Department of Mining Engineering, Faculty of Environment, Urmia University of Technology, Urmia, Iran
2. Assistant Professor, Department of Mining Engineering, Faculty of Environment, Urmia University of Technology, Urmia, Iran
3. Ph.D. Candidate, Department of Civil Engineering, University of Calabria, 87036 Rende, Italy
4. Professor, Department of Mining, Petroleum & Geophysics Engineering, Shahrood University of Technology, Shahrood, Iran
5. M.S., Department of Civil Engineering, Faculty of Environment, Urmia University of Technology, Urmia, Iran
6. Ph.D. Candidate, Department of Mining and Metallurgical Engineering, Yazd University, Yazd, Iran
7. Professor, Department of Civil Engineering, Korea Maritime and Ocean University, Pusan 49112, Korea
8. Associate Professor, College of IT Convergence, Gachon University, Seongnam 13120, Korea
Corresponding author: *geem@gachon.ac.kr*

https://doi.org/10.22115/SCCE.2022.325638.1398

ARTICLE INFO

ABSTRACT

Freezing is one of the most effective natural and environmental factors on the physical and mechanical characteristics of dimension stones. Since, freezing is a destructive agent, thus causes the undesirable stone conditions and reduces quality and its efficiency. This study, it was aimed to evaluate and rank the dimension stones according to their changes in physical and mechanical properties due to freezing conditions. For this purpose, 14 rock types of the most widely used dimension stones in cold regions were collected and transferred to the laboratory to determine their physical and mechanical characteristics. In laboratory tests, standard samples of stones were prepared, and for all of the samples Uniaxial Compressive Strength (UCS), Durability Index (DI), Density (D), and Water absorption percentage (Wa) were determined before and after different freezing–thawing cycles. Then utility degree of studied stones in frost condition was assessed using the preference ranking organization method for enrichment of evaluations (PROMETHEE) multi-criteria decision-making method. The results of the study showed that samples of A3 (Piranshahr Granat), A10 (Hamadan black granite), A8 (Azarshahr yellow travertine), and A4 (Mahabad gray granite) are in order from the highest degree of desirability in a condition of freezing–thawing and for use in cold climates are especially suitable for use in outdoor and urban spaces. In addition, the results of the laboratory were evaluated by the PSO algorithm for clustering analysis and com-pared with the ranking result by PROMETHEE. The results obtained demonstrated the proposed approach could be an efficient tool in the evaluation of the freezing phenomenon on physical and mechanical properties of dimension stones.

---

1. Introduction

One of the most important factors that influences the efficiency of industrial activities is climate-related factors [1]. Temperature, as one of the climatic factors, has the greatest impact on mining activities, so that mining operations may be stopped in the event of severe temperature changes [2]. On the other hand, temperature changes cause the resistance of rocks to change [3]. Iran, located in Middle East, is famous for a diverse climate in the whole world that rapid temperature changes, the differences between hottest and coldest temp. During the day, hot sun and long freezes are sometimes diverse and conflicting climate properties of Iran [4]. The northwest and western provinces of Iran have mild summer and cold winters [5]. The high rainfall and cold climate are characteristics of the winter in these regions, and since the major potential and vast resources of decorative stones are located in these regions, stone owns a special place in the culture and art of housing in these regions. According to difficult climate conditions, facade stones suffer long-term freezing and multiple freezing–thawing cycles. This causes erosion and vast destruction of a variety of dimension stones of structures and reduces life and beauty [6,7]. A wide study on the effectiveness of freezing and thawing at the international level on the physical and mechanical properties of stones has taken place [8,9].

Many research works have been accomplished for the study of the impacts of freeze–thaw cycles on the physical and mechanical characteristics of dimension stones. Matsuoka (1990) studied the effectiveness of the freezing–thawing cycle according to water content in the stone [10]. In this regard, Nicholson and Nicholson (2000) inspected on decline mode for ten types of sedimentary rocks according to recrudescent cycles of freeze–thaw process [11]. In other studies, Mutluturk et al. (2004) offered a model to study the decay of stone during freezing–thawing cycles [12]. Then, Altindag et al. (2004) inspected it for the entirety damage of ignimbrite and specified the impacts of freeze–thaw cycles on Isparta ignimbrite, and this model was evaluated by these researchers[13]. Chen et al. (2004) study the welded porous of tuff from the viewpoint of the effect of water saturation to freeze–thaw cycles. The results indicate that both porosity and rock degrading significantly enhance when the saturation degree exceeds 70% [14]. Karaca (2010) inspected experimentally the effect of freeze–thaw cycles on the abrasion values [15]. Tan et al. (2011) studied the effect of freezing–thawing cycles on stone mechanical characteristics [16]. Also, Bayram (2012) presented a novel statistical model for estimating the percentage damage value in the uniaxial compressive strength of nine limestone examples after a freeze–thaw test [17]. Vehbi Gökçe et al. (2016) reviewed the impact of the number of freezing–thawing cycles on physical and mechanical travertine characteristics using statistical studies made in Turkey [18]. The research was done in Iran in regard of effect of freezing and thawing on physical and mechanical properties of dimension stones, studies of Jamshidi et al. (2013), and also researches of Khanlari et al. (2015) in Iran, can be noted [19,20]. Cyclic freeze–thaw event in the cold and wet areas, change mechanical and physical characteristics of rocks. When water freezes, its volume increases up to 9%, and consequently by erecting dividing force on the sidewall of fractures and pores, increases pore pressure [21]. New discontinuities create or old fissure developed when pressure passes the level of the tensile strength of the rock pore; as a result, these changes can affect the stone's mechanical strength and thus its durability [22,23]. Also, Jamshidi et al. (2016) presented a new physicomechanical index for predicting the mechanical

strength of travertine after a freeze–thaw test. The results of this research indicated that the physicomechanical parameter is well precise for predicting the mechanical strengths of travertine such as, uniaxial compressive strength and point load strength and Brazilian tensile strength after a freeze–thaw test, and consequently present a rapid durability evaluation [24]. In the other studies, Li et al. (2018) examined the time-dependent behavior of quartz sandstone and quartzite according to chemical degradation and freeze–thaw cycles [8]. Liping et al. (2019) were studied the physical index change and triaxial compression test of intact hard rock subjected to freeze-thaw cycles [25]. In another study, Peng et al. (2020), were evaluated the effect of rock freeze-thaw in cold-region tunnels [26]. Also, a deformation property of coarse-grained sulfate saline soil based on the freeze-thaw-precipitation cycle was studied by Zhang et al. (2020) [27].

In all these studies, researchers aimed to evaluate and research the coherence between different cycles of freezing and thawing and physical and mechanical properties of dimension stones which has resulted in valuable results. This study aimed in addition to evaluate the effect of quantity of freezing on most widely used dimension stones of the country, degree of desirability of studied stones using the PROMETHEE method. So that the most desirable dimension stone for use in urban structures is determined and provides a clear vision about its impact on the stone selection. It must be noted that there has not been much research on the ranking of dimension stones in different freezing–thawing cycles. Therefore, the necessity of research in this regard is undeniable. It should be noted that extensive studies have been done on the use of the PROMETHEE method in evaluating various mining engineering problems, some of which are mentioned in Table 1.

Table 1
Some of the studied using the PROMETHEE method [28,29,38–44,30–37].

Researcher(s)	Year	Description
Dağdeviren	2008	Equipment selection
Athawale & Chakraborty	2010	Facility location selection
Prvulovic et al.	2011	Choice of systems for drying paltry-seeds and powder materials
Bogdanovic et al.	2012	Mining method selection
Abedi et al.	2012	Copper exploration
Shiriskar & Patil	2013	Optimization of energy charges
Balali & Zahraie	2014	Selection of building structural system
Mikaeil et al.	2015	Sawability of dimension stone
Mladineo et al.	2016	Priority setting in management of mine action projects
Balusa & Singam	2018	Underground mining method selection
Mikaeil et al.	2018	Geotechnical risks assessment in tunneling projects
Ghadernejad et al.	2019	Selection of optimal coal seam
Iphar & Alpay	2019	Underground mining method selection
Sitorus et al.	2019	Choice problem in mining and mineral processing
Mikaeil et al.	2020	Evaluating the coal seam mechanization
Dayo-Olupona et al.	2020	Selection of emerging technology in surface mines
Dachowski & Gałek	2020	Selection of the Best Method for Underpinning Foundations

According to the results of research conducted with the PROMETHEE method (Table 1), it can be said that this method can evaluate and rank in solving various problems of mining engineering. On the other hand, the results of the research show that this method is compatible with real-world conditions and provides reliable results for researchers and designers of mines.

2. Field and laboratory studies

This research contained two main parts as field and laboratory studies. In the field study, rock samples are provided from studied quarries located in Iran. In the laboratory study, the characteristics of physical and mechanical are determined before and after freeze–thaw cycling. Finally, the desirability degree of studied dimension stones is deter-mined using the PROMETHEE method and clustering technique. The flowchart of the re-search procedure is illustrated in Figure 1.
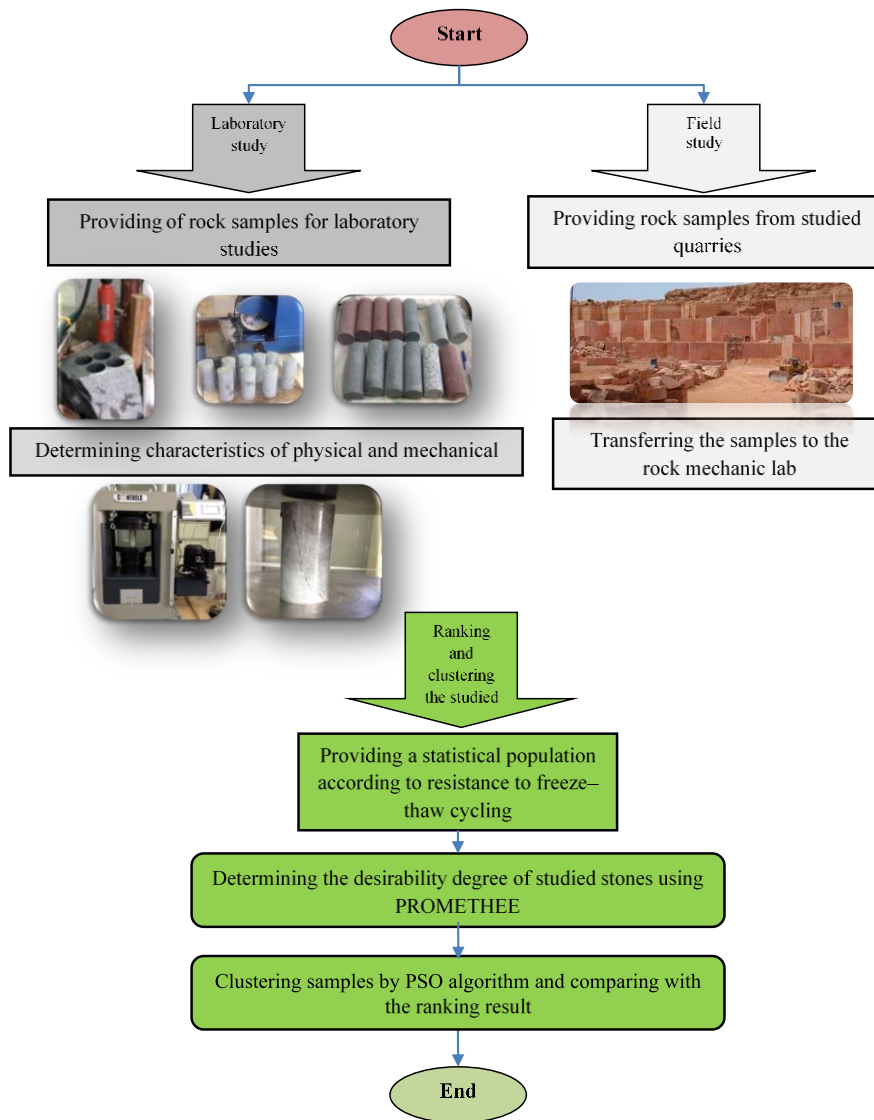

Fig. 1. Flowchart of the study.

In this study, the numbers of dimension stones of west and northwest regions of Iran are checked. Frequency, locality, beauty, color, and price for these stones are the reason. So, 14 dimension stones are selected. The studied dimension stones are given in Table 2. The location of the studied quarries is shown in Figure 2.

Table 2
Studied dimension stones.

Sample ID	Rock-type	City	Province
A_1	Cream travertine	Khalkhal	Ardabil
A_2	Walnut travertine	Azarshahr	East-Azerbaijan
A_3	Olive granite	Piranshahr	West-Azerbaijan
A_4	Gray granite	Mahabad	West-Azerbaijan
A_5	Red granite	Naein	Isfahan
A_6	Spring White granite	Zanjan	Zanjan
A_7	White travertine	Tekab	West-Azerbaijan
A_8	Yellow travertine	Azarshahr	East-Azerbaijan
A_9	Red marble	Azarshahr	East-Azerbaijan
A_{10}	Black granite	Hamadan	Hamadan
A_{11}	Chocolate granite	Khoramdare	Zanjan
A_{12}	Cream marble	Harsin	Kermanshah
A_{13}	Cream Pink travertine	Anarak Chopanan	Isfahan
A_{14}	Pink marble	Anarak Haftoman	Isfahan

Fig. 2. Flowchart of the study.

According to the nature of the freezing experiment, the need to control the uniformity of samples is of utmost importance. So, in this research to ensure the accuracy of the samples and to obtain uniform samples, instead of gathering samples from quarries, samples from stones factories in

Tabriz city were collected and transported to the rock mechanic laboratory. In total, a block with an average size of $40\times40\times50$ cm^3 was selected from each type of stone. To begin studies in the laboratory, the 8 NX diameter cores and a length to diameter ratio of 5/2 were prepared. In all experiments, all steps have been according to Laboratory ISRM Standards [45]. According to ISRM, freezing experiment is performed at a temperature of –15ºC, however in this study, considering that at least 20 nights a year at some of the cities in West and northwest of the country temperature reach –20ºC even less, therefore, the temperature suitable for the simulation and realistic study of stones, laboratories were asked to test freezing and thawing in 5 courses at a temperature of –20ºC. All tests were done once on the control samples and the samples which were spent freezing test and a week normally lost their moisture. It should be noted that the five of experiments for each sample before and after the freezing–thawing were conducted and the average of the results for each sample are shown in Table 3. Also, the results of tests on stone samples before and after the freezing–thawing are given in and Figures 3 to 6.

Table 3
Physical and mechanical properties of the studied stones before and after the freezing-thawing.

Sample ID	D (gr/cm^3)		Wa (%)		UCS (MPa)		DI (%)	
	Before freezing	After freezing	Before freezing	After freezing	Before freezing	After freezing	Before freezing	After freezing
A_1	2.46	2.38	2.1	2.8	50.5	43.5	97.69	96.12
A_2	2.52	2.48	2.72	2.95	48.5	41	98.87	97.67
A_3	3.18	3.13	0.41	0.43	105.5	95.5	99.38	98.68
A_4	3.23	2.98	0.30	0.31	189	182.5	99.57	98.07
A_5	3.31	2.87	1.02	1.1	177.5	169	99.72	98.86
A_6	2.87	2.69	0.96	1.05	121	111.5	99.43	98.49
A_7	3.06	3	1.56	1.81	89	82.5	98.73	97.64
A_8	2.56	2.31	2.61	2.76	33	32	98.43	97.29
A_9	2.6	2.43	2.54	2.63	52.5	48	99.12	98.18
A_{10}	3.26	3.01	0.25	0.265	173	166.5	99.56	98.88
A_{11}	2.95	2.74	0.98	1.05	133	126.3	99.31	98.1
A_{12}	2.86	2.6	1.57	1.7	71.5	62	98.79	97.94
A_{13}	3.07	2.72	1.94	2.03	73	65.5	99.14	98.23
A_{14}	3.23	3.094	1.2	1.305	74.5	68	99.42	97.93

D: Density, ***Wa***: Water absorption percentage, ***UCS***: Uniaxial compressive strength, ***DI***: Durability index

As can be seen in Table 3, freezing–thawing more seriously affects the mechanical and physical properties of stones. Two important physical properties such as density and water absorption properties seem to be more effective by freezing–thawing. When the stones are wet, water permeates in stone pores and micro-cracks and causes freezing and the volume increase of existing water in these spaces increases internal tensions and affects the macroscopic structure of the stone. With ice thawing in these spaces, the structure of the stone releases from ice pressure, and very mild tension relief is created in the stone. This phenomenon increases stone micro-cracks and gets flaky inside and outside. A rapid freezing–thawing cycle toughens up the destruction of freezing. All the process alters the physical properties of stone, especially the two mentioned parameters and decreases in mechanical properties including compressive strength and durability index.
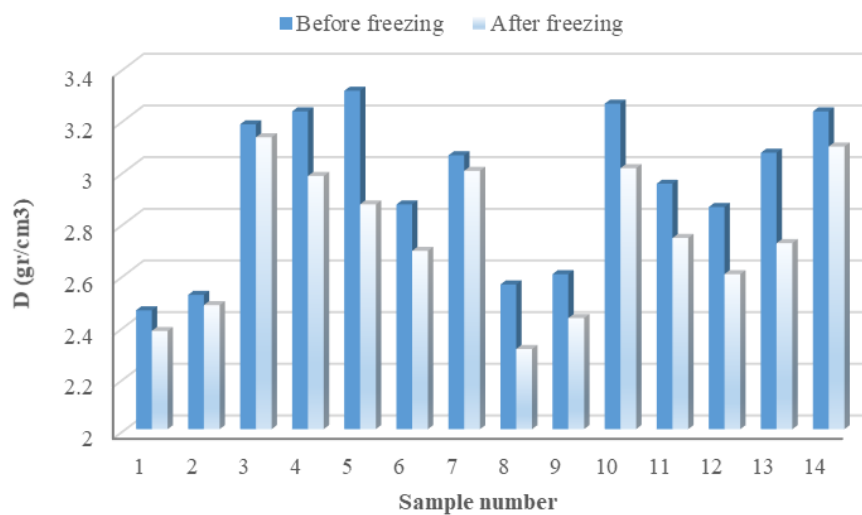

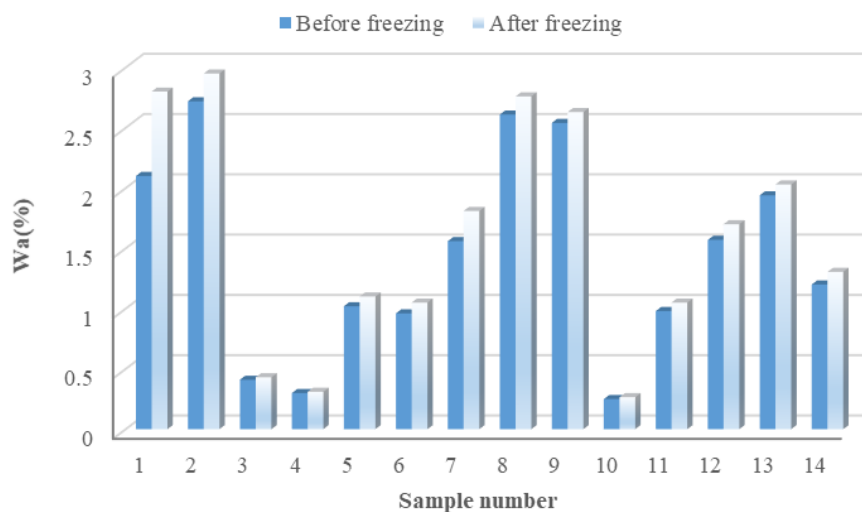**Fig. 3.** The effect of the freezing–thawing on density.

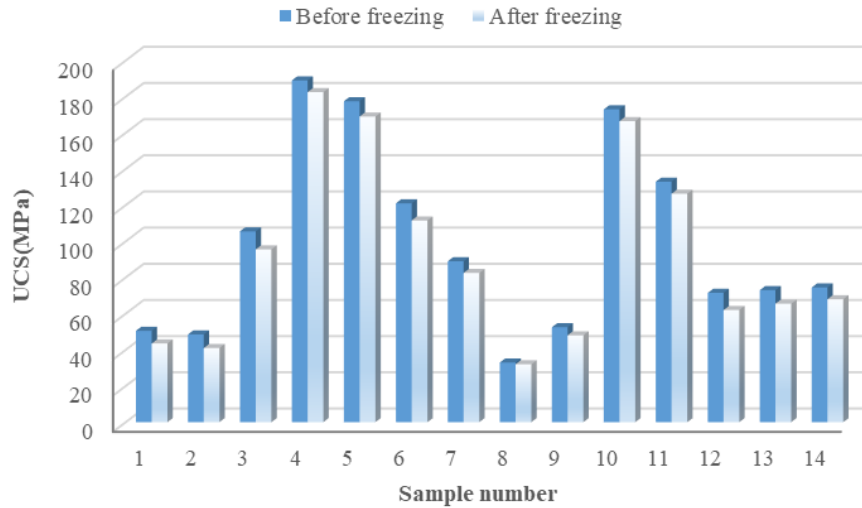**Fig. 4.** The effect of the freezing–thawing on water absorption percentage.

Fig. 5. The effect of the freezing–thawing on uniaxial compressive strength.
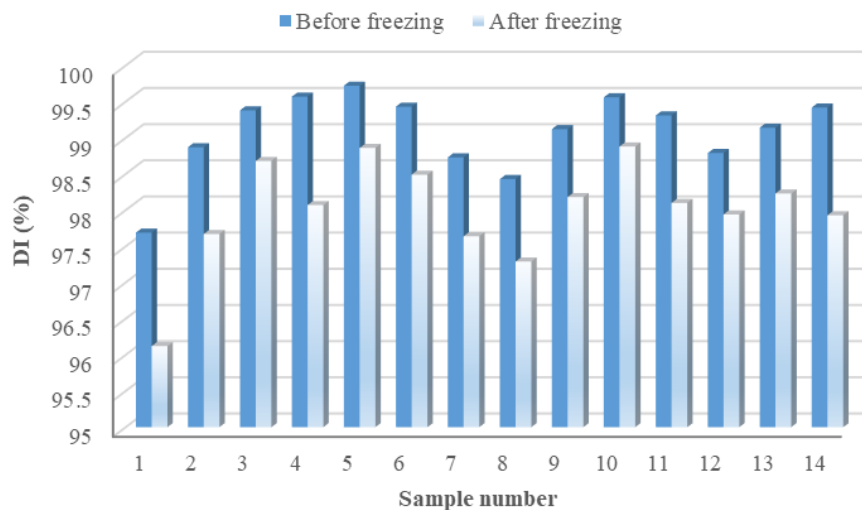

**Fig. 6.** The effect of the freezing–thawing on durability index.

As can be seen in Table 3, the effects of freezing-thawing on the physical and mechanical characteristics are clear. After freezing-thawing, density, durability index, and uniaxial compressive strength are decreased and water absorption is increased. The percentage changes of studied parameters affected by freezing-thawing are given in Table 4 and Figure 7.

As seen in Table 4, A5(Naein red granite) with a 13% reduction in the density highest, and A2 (Azarshahr walnut travertine) and A3 (Piranshahr olive granite) have the lowest density reduction. Also, the average density of stones decreased by 7.02% due to freezing. It can be seen that A1 (Khalkhal cream travertine) with 33%, the highest, and A4 (Mahabad gray granite) by 3%, have the lowest increase water absorption, on average, water absorption percentage in the studied stones by freezing is 9.01%.

Table 4
Physical and mechanical properties percentage changes of studied stone after freezing-thawing.

Sample ID	Change (%)			
	D	Wa	UCS	DI
A_1	−3	33	−13.86	−1.6
A_2	−2	8	−15.46	−1.21
A_3	−2	5	−6.63	−0.7
A_4	−8	3	−3.43	−1.5
A_5	−13	8	−4.78	−0.86
A_6	−6	9	−7.85	−0.94
A_7	−2	16	−7.3	−1.1
A_8	−10	6	−3.03	−1.16
A_9	−7	4	−8.57	−0.95
A_{10}	−7.6	6	−3.75	−0.6
A_{11}	−7.1	7	−5.03	−1.22
A_{12}	−9	8	−13.28	−0.86
A_{13}	−11.4	4.5	−10.27	−0.91
A_{14}	−4.2	8.7	−8.72	−1.49
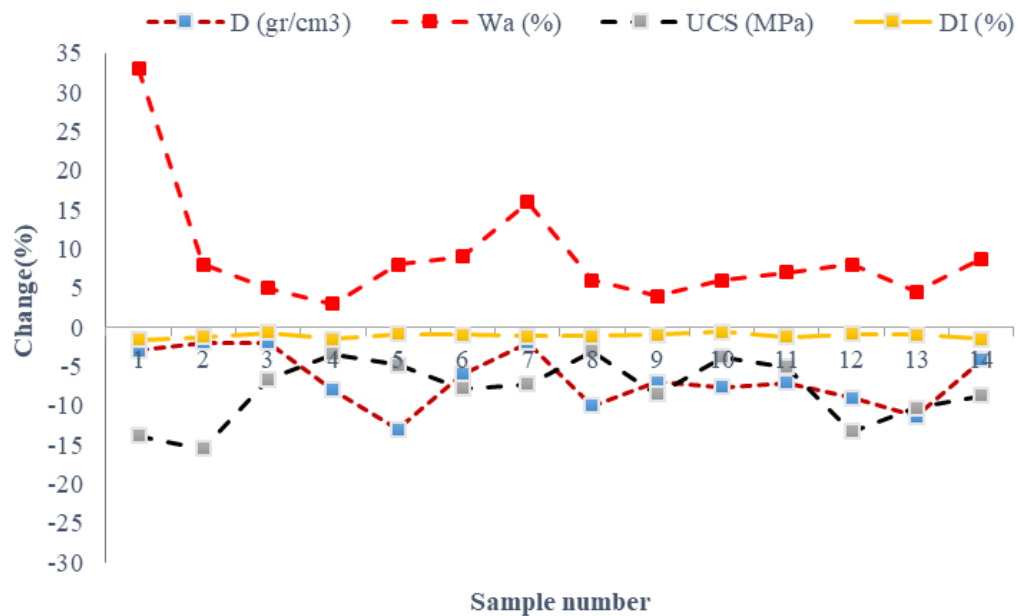
Fig. 7. The percentage changes of studied parameters after freezing-thawing.

Also, according to Table 4, A2 (Azarshahr walnut travertine) with 15.46%, the highest reduction in compressive strength, and A8 (Azarshahr yellow travertine) with 3.03%, have the lowest decrease in compressive strength in the effect of freezing. The mean decrease in the compressive strength of stones in the effect of freezing is 8.01%. Also, A1 (Khalkhal cream travertine) with a 1.57 drop in durability index has the highest, and A10 (Hamadan black granite) with a 0.6%, has the lowest decrease in durability index, in the effect of freezing the durability index drops into 1.07% on average.

3. Determining the desirability degree of studied stones using PROMETHEE

The PROMETHEE is a method for making multi-criteria decisions as an efficient solves method, using two words preferred and indifference to choose the best option. The method is applied in many fields of engineering such as operations research and dynamic management. This method has been well-attended because of its mathematical properties and its ease of use. According to the PROMETHEE method (Eq 1):

$$Max\ (Min)\{f_1(a), f_2(a),...,f_k(a) \mid a \in A\} \tag{1}$$

A represents a set of decision options.

The $f_j(a)$ shows (j) indicator value in option a, and $j = 1, 2,..., k$ is the set of indicators or criteria that evaluates the options. Rating options by comparing the test is done on each indicator that this ranking is done in three steps as follows [42]:

First step: Compare options using a pre-defined preference function with $[0, +1]$ domain. For example, the preference function P, to examine options a and b and j indicator is as follows:

$$P_j(a,b) = P_j\left[d_j(a,b)\right] \tag{2}$$

So that: $d_j(a,b) = f_j(a) - f_j(b)$ represents the difference in the J indicator. Of course, for each fj indicator a weight (wj) also is considered.

Second step: Calculating the overall preference of $\pi(a,b)$ or each option. The higher $\pi(a,b)$, the more preferable. The value of $\pi(a,b)$ is calculated as follows:

$$\pi(a,b) = \sum_{j=1}^{k} w_j . p_j(a,b) \tag{3}$$

Where: $\sum_{j=1}^{k} w_j = 1$, and J is weight indicator (w_j).

Third step: Calculating the overall preference of option a on other options. In this section output flow and also preferred the other choices on the option a is calculated as follows:
for positive or output flow ratings:

$$\Phi^+(a) = \frac{1}{n-1}\sum_{x \in A} \pi(a, x) \tag{4}$$

It shows how much priority an option a has over others. It shows the real power of option a. The $\Phi^+(a)$ largest amount means the best option.
for negative input flow ratings:

$$\Phi^-(a) = \frac{1}{n-1}\sum_{x \in A} \pi(x, a) \tag{5}$$

This shows that other options to what extent have priority over option *a*. In reality, this shows option *a*'s weaknesses. The smallest $\Phi^-(a)$ represents the best option.

Minor ratings of options can be done by positive or negative flow PROMETHEE I.

For complete rankings of all options the net flow ranking must be defined for each option PROMETHEE II:

$$\Phi(a) = \Phi^+(a) + \Phi^-(a) \tag{6}$$

The resulting flow balance of positive and negative and net flow ranking higher, indicating a better option. For ranking and determining the desirability of studied stones by PROMETHEE the steps are to follow:

Step 1. Forming decision matrix: This matrix indicates studied stones and their percentage change in density, water absorption, durable creep, and uniaxial compressive strength during different freezing–thawing cycles (Table 4).

Step 2. Forming normalized decision matrix: For normalizing the data relating the value of each element is divided into the square root of the sum of squared elements in each column. The normalized decision is shown in Table 5.

Table 5
Normalized decision matrix.

Sample ID	D	Wa	UCS	DI
A_1	0.108	0.760	0.417	0.384
A_2	0.072	0.184	0.465	0.290
A_3	0.072	0.115	0.199	0.168
A_4	0.287	0.069	0.103	0.359
A_5	0.467	0.184	0.144	0.206
A_6	0.215	0.207	0.236	0.226
A_7	0.072	0.369	0.220	0.264
A_8	0.359	0.138	0.091	0.276
A_9	0.251	0.092	0.258	0.226
A_{10}	0.273	0.138	0.113	0.143
A_{11}	0.255	0.161	0.151	0.291
A_{12}	0.323	0.184	0.400	0.205
A_{13}	0.409	0.104	0.309	0.217
A_{14}	0.151	0.200	0.262	0.356

Step 3. Forming weighted normalized decision matrix: Each element in relating column in normalized matrix multiplied in the weight of every indicator. In this part the weight is assumed variable. Table 6 indicates the equal weight index weighted normalized decision matrix.

Table 6
Weighted normalized decision matrix.

Sample ID	D	Wa	UCS	DI
A_1	0.027	0.190	0.104	0.096
A_2	0.018	0.046	0.116	0.072
A_3	0.018	0.029	0.050	0.042
A_4	0.072	0.017	0.026	0.090
A_5	0.117	0.046	0.036	0.051
A_6	0.054	0.052	0.059	0.056
A_7	0.018	0.092	0.055	0.066
A_8	0.090	0.035	0.023	0.069
A_9	0.063	0.023	0.064	0.057
A_{10}	0.068	0.035	0.028	0.036
A_{11}	0.064	0.040	0.038	0.073
A^{12}	0.081	0.046	0.100	0.051
A_{13}	0.102	0.026	0.077	0.054
A_{14}	0.038	0.050	0.066	0.089

Step 4. Calculating $P_j(a,b)$ and $\pi(a,b)$: In this part after calculating differences of options, the amount $P_j(a,b)$ for each of the options about each indicator according to the first function would be achieved. In continue values for the options were calculated according to overall priority. The results of this review for option 1, according to Eqs 2 and 3, are shown in Table 7.

Table 7
Option 1 comparison with other options using the first $\pi(a,b)$ function with the value.

	D	Wa	UCS	DI	$\pi(a,b)$
(A_1,A_2)	0.009	0.144	− 0.012	0.023	0.75
(A_1,A_3)	0.009	0.161	0.054	0.054	1
(A_1,A_4)	− 0.045	0.173	0.078	0.006	0.75
(A_1,A_5)	− 0.090	0.144	0.068	0.044	0.75
(A_1,A_6)	− 0.027	0.138	0.045	0.040	0.75
(A_1,A_7)	0.009	0.098	0.049	0.030	1
(A_1,A_8)	− 0.063	0.155	0.081	0.027	0.75
(A_1,A_9)	− 0.036	0.167	0.040	0.039	0.75
(A_1,A_{10})	− 0.041	0.155	0.076	0.060	0.75
(A_1,A_{11})	− 0.037	0.150	0.066	0.023	0.75
(A_1,A_{12})	− 0.054	0.144	0.004	0.045	0.75
(A_1,A_{13})	− 0.075	0.164	0.027	0.042	0.75
(A_1,A_{14})	− 0.011	0.140	0.039	0.007	0.75

Step 5. Calculating minor ranking input and output flow: For selecting the best option, n–1 options of *A* collection must be rejected. For this purpose, two priority flows are defined. Prioritizing output flow shows how much each choice has priority over other choices. Prioritizing input flow also shows how much of a particular option is superior to other options. So, the largest output and lowest input belong to the best option. Results of calculating the prioritized using Eqs 4 and 5 are shown in Table 8.

Step 6. The net flow calculation and rating options: PROMETHEE I method calculates net flow options rating and represents each option's superiority over other options. In this case, larger net flow represents the option's superiority. The result of the calculation of net flow

prioritization using Eq 6 and ranking of studied dimension stones are shown in Table 8, Figures 8 and 9.

Table 8
Input and output flow and net flow and final options ranking.

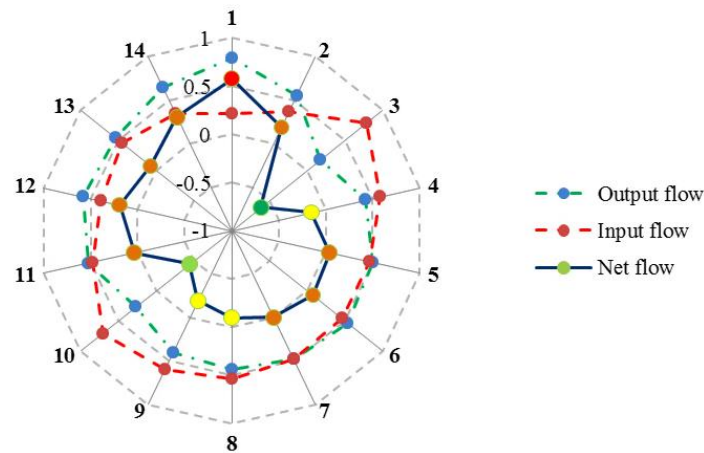| Sample ID	Output flow (positive)	Input flow (negative)	Net flow	Ranking
A_1	0.788	0.212	0.577	11
A_2	0.558	0.365	0.192	9
A_3	0.173	0.788	− 0.615	1
A_4	0.423	0.577	− 0.154	4
A_5	0.500	0.462	0.038	7
A_6	0.538	0.462	0.077	8
A_7	0.481	0.481	0	6
A_8	0.442	0.538	− 0.096	5
A_9	0.404	0.596	− 0.192	3
A_{10}	0.269	0.712	− 0.442	2
A_{11}	0.519	0.481	0.038	7
A_{12}	0.577	0.385	0.192	9
A_{13}	0.538	0.462	0.077	8
A_{14}	0.654	0.346	0.308	10

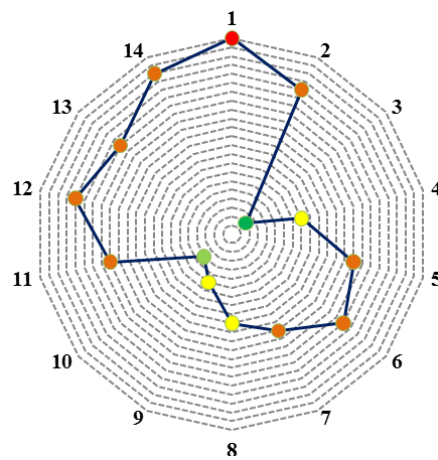**Fig. 8.** Input, output, and net flow of studied dimension stones.

Fig. 9. Ranking of studied dimension stones.

...

As mentioned, indicators had the same importance. To review indicators' importance in ranking in studied samples, sensitivity in indicators weight is considered. The results of the review showed in 13 states shown in Table 9.

Table 9
Ranking the options according to different weights assigned to the indicator.

	Indicators weight												
D	0.25	0.500	0.750	1	0.166	0.084	0	0.167	0.083	0	0.167	0.083	0
Wa	0.25	0.167	0.083	0	0.05	0.750	1	0.166	0.084	0	0.187	0.083	0
UCS	0.25	0.167	0.083	0	0.167	0.083	0	0.500	0.750	1	0.166	0.084	0
DI	0.25	0.166	0.084	0	0.167	0.083	0	0.167	0.083	0	0.500	0.750	1
Sample ID	Net flow												
A_1	0.577	0.205	−0.167	−0.538	0.719	0.858	1	0.666	0.757	0.846	0.718	0.859	1
A_2	0.192	−0.154	−0.500	−0.846	0.206	0.217	0.231	0.461	0.731	1	0.266	0.321	0.385
A_3	−0.615	−0.699	−0.770	−0.846	−0.590	−0.564	−0.538	−0.487	−0.359	−0.231	−0.693	−0.769	−0.846
A_4	−0.154	0.024	0.206	0.385	−0.436	−0.718	−1	−0.384	−0.616	−0.846	0.180	0.512	0.846
A_5	0.038	0.359	0.679	1	0.102	0.168	0.231	−0.154	−0.346	−0.538	−0.153	−0.347	−0.538
A_6	0.077	−0.025	−0.129	−0.231	0.282	0.487	0.692	0.076	0.078	0.077	−0.026	−0.128	−0.231
A_7	0	−0.282	−0.564	−0.846	0.283	0.564	0.846	−0.026	−0.050	−0.077	0.026	−0.128	0.077
A_8	−0.096	0.166	0.430	0.692	−0.167	−0.236	−0.308	−0.397	−0.699	−1	0.014	0.121	0.231
A_9	−0.192	−0.154	−0.115	−0.077	−0.410	−0.628	−0.846	−0.051	0.089	0.231	−0.154	−0.115	−0.077
A_{10}	−0.442	−0.218	0.006	0.231	−0.398	−0.352	−0.308	−0.526	−0.609	−0.692	−0.628	−0.815	−1
A_{11}	0.038	0.051	0.065	0.077	0	−0.038	−0.077	−0.102	−0.244	−0.385	0.205	0.372	0.538
A_{12}	0.192	0.308	0.422	0.538	0.205	0.218	0.231	0.359	0.526	0.692	−0.103	−0.397	−0.692
A_{13}	0.077	0.334	0.590	0.846	−0.180	−0.435	−0.692	0.231	0.384	0.538	−0.077	−0.230	0.385
A_{14}	0.308	0.077	−0.154	−0.385	0.385	0.461	0.538	0.333	0.359	0.385	0.436	0.564	0.692

4. Particle Swarm Optimization

In recent decades, artificial intelligence (AI) techniques, have played a significant role in solving complex problems in industry and science in theory and practice [46–53]. Numerous studies were conducted in a wide range of sciences that demonstrated the practical applications of these methods [54–59]. The Particle Swarm Optimization (PSO) is one of the most widely used and effective algorithms in solving various problems in conditions of uncertainty, which can be considered in the Swarm Intelligence (SI) which was first proposed by Kennedy and Eberhart (1995) [60]. This algorithm is based on the pattern of mass movement of fish in water or birds during migration to find its way to evolution and achieve the most optimal answer or answers. In this algorithm, starting with the optimization process, a set of particles (answers) are generated randomly. These particles move in set to get the best possible position in a D-dimensional space [61–63]. Each particle is represented by two vectors of position and velocity that represent the direction of its flight and velocity based on Figure 11.
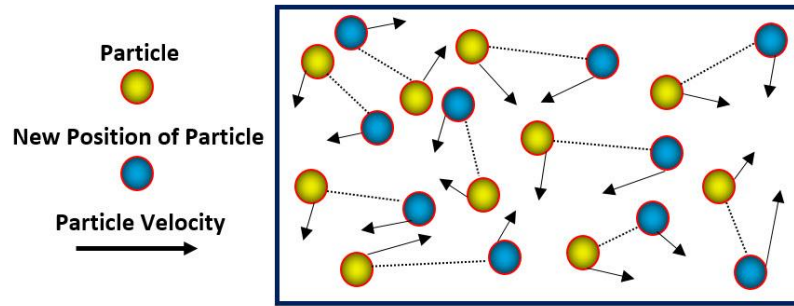
Fig. 11. New velocity and position vectors of a set of particles.

Each particle, after moving at any moment, the velocity and position vectors are updated according to Eqs 7 and 8, respectively. Two components of the velocity vector are the personal best position (Pbest) and global best position (Gbest).

$$V_i^{(k+1)} = wV_i^k + c_1 r_1.(pbest_i - X_i^k) + c_2 r_2.(gbest - X_i^k)$$ (7)

$$X_i^{(k+1)} = X_i^k + V_i^k$$ (8)

Where $V_i^{(k+1)}$, and $X_i^{(k+1)}$ represent the new velocity vector, and new position. Also, V_i^k, and X_i^k express the initial velocity vector and position of particles. The r_1 and r_2 are random numbers with uniform distribution with a range between 0 and 1. The w expresses the inertia weight to ensure convergence in the particle set. In addition, c_1 and c_2 are positive constants that called the individual learning factor and the social learning factor, respectively. Generally, the values of c_1 and c_2 are considered equal to 2, while Eq 9 must be met [64,65].

$$c_1 + c_2 \leq 4$$ (9)

Position and velocity vectors of particles constantly being updated, and the optimization process is stopped when the best possible answer is achieved. It is worth mentioning that the PSO algorithm is used to train other algorithms such as artificial neural networks, neuro-fuzzy inference systems, and support machine vectors. Hence, in this study, the particle algorithm is used in training the Lloyd algorithm for clustering and data analysis, which is described in the following section.

5. Clustering model and discussion

As mentioned earlier, the PSO has a wide range of applications. Therefore, in this study, the PSO is employed to train Lloyd's algorithm (k-means clustering). Clustering is one of the most effective methods in data analysis that the particle algorithm with the training of the Lloyd algorithm (one of the most popular clustering algorithms) increases the ability to classify analyze data to a desirable level [66]. Lloyd's algorithm is considered as a fitness function that is shown in Eq 10.

$$Obj.Function = \sum_{i=1}^{n} \min_{1 \le j \le k} d(x_i, m_j) \qquad (10)$$

Where $d(x_i, m_i)$ represents the Euclidean distance of each member from each class's center. j expresses the amount of clusters $j=(1,2,3,\dots,k)$[67–69].

For maximum algorithm efficiency in data analysis, the algorithm's control parameters must be determined that play an effective role in algorithm convergence. Since there are no specific relationships to determine these control parameters, a set of these parameters were selected based on previous studies [70–72]. Then, according to the data set and after trial and error, the most appropriate ones were selected including the number of clusters c=2, minimum acceptance precision of $\varepsilon L=0.00001$, the initial population of 100, and maximum iteration of 150. The rock samples are classified into two classes based on the amount of physical and mechanical properties percentage changes after freezing-thawing. The results of this classification are demonstrated in Table 10 and compared with the results of ranking the rocks based on the permutation method.

Table 10
Comparison of the results of clustering by PSO in two classes with the results of ranking by PROMETHEE.

Sample ID	Clustering by PSO	PROMETHEE technique	
		Ranking	Net flow
A_1	2	11	0.577
A_2	1	9	0.192
A_3	1	1	− 0.615
A_4	1	4	− 0.154
A_5	1	7	0.038
A_6	1	8	0.077
A_7	1	6	0
A_8	1	5	− 0.096
A_9	1	3	− 0.192
A_{10}	1	2	− 0.442
A_{11}	1	7	0.038
A_{12}	1	9	0.192
A_{13}	1	8	0.077
A_{14}	1	10	0.308

According to Table 3, the results of clustering by PSO algorithm showed that the rock sample A1 was classified alone in one class and the other samples in another class together. Also, in a comparison with the results obtained from the PROMETHEE method, it is determined that the sample of A1, which is classified separately in the second class, has the lowest rank and has the highest amount of net flow compared to other samples.

Finally, the following remarks can be concluded:

The results of the experiments showed that after freezing density, uniaxial compressive strength, and durability index of stone are reduced and water absorption is increased. The reason for these changes can be analyzed in continuous periods of freezing and thawing that process of freezing and thawing sequence created and a series of large and small joints and cracks in the stone. However, if the joints and cracks appear on the surface small pieces of stone sometimes appear in the form of powder. If the cracks are within the volume of stone and the stone porosity is increased. The combination of these states reduces mass and increases the volume of sample stones and finally, characteristics such as density, strength, and durability of stone are decreased. Also, due to the formation of cracks in the stone, stone absorbs more water in free spaces and water absorption is increased. Studies on the rock-mechanical test of stone samples showed that A5 (Naein red granite) with 13% decrease in density is highest and three walnut travertine, A3 (Piranshahr Granat) and A7 (Tekab White travertine) with 2% have lowest density decrease during freezing. Also, in average stones density in freezing conditions decreased by 7.02%. Differences between the highest and lowest density percentage among studied stones were 11%. A1 (Khalkhal cream travertine) with 33% increase and A4 (Mahabad gray granite) with 3%, in order, had the highest and lowest water absorption percentage increase. On average, the water absorption percentage showed a 9.01% increase in freezing conditions. Differences between the highest and lowest water absorption percentages among studied stones were 3%. A2 (Azarshahr walnut travertine) with 15.46% and A8 (Azarshahr yellow travertine) with 3.03 in order had highest and lowest compressive strength in freezing condition. The average reduction in stones compressive strength was 8.01. Also, A1 (Khalkhal cream travertine) with 1.57% durability Index drop was highest and A10 (Hamadan black granite) with 0.6% had the lowest drop and in average durability index in freezing condition drops by 1.07. Then, using PROMETHEE multi-criteria decision-making with varied weights, the 14 samples were used to determine the degree of desirability of the stones. In most circumstances, the options A3, A10, A8, and A4 have the maximum degree of freezing–thawing desire. Finally, classifying of laboratory data using PSO algorithm and comparison with the results of PROMETHEE ranking showed that the used methods can be considered as a suitable tool for assessing dimension stone according to resistance to freeze–thaw cycling to use in cold regions.

6. Conclusions

Freezing is one of the most effective environmental factors to the physical and mechanical properties of dimension stones. Since freezing is a destructive agent, thus causes the undesirable stone conditions and reduces quality and its efficiency. In this study, freezing effects on the physical and mechanical dimension stones were evaluated and the desirability degree of these

stones was ranked according to four percentage changes of important physical and mechanical such as density, water absorption, uniaxial compressive strength, durability index. For this purpose14 rock types of the most widely used dimension stones in cold regions were collected and transferred to the laboratory. To analyze the actual conditions of freezing in the cold areas that face freezing in winter, stones were studied at –20ºC. Determining the degree of desirability studied stones using PROMETHEE multi-criteria decision-making with different weights for the 14 cases studied and evaluated. The results of this study showed that in most cases the option A3 (Piranshahr Granat), A10 (Hamadan black granite), A8 (Azarshahr yellow travertine), and A4 (Mahabad gray granite) have the highest degree of desirability in terms of freezing–thawing. Thus, sample stones of A3, A10, A8, and A4 are the most desirable stones in cold climates among studied stones. Then, the results of the laboratory were classified by PSO algorithm and compared with the results of PROMETHEE. Consequently, it could be recognized as the lowest rank in a separate class. This study indicated that the proposed approach can be applied as a reliable tool for evaluating freezing phenomena in rock mechanics engineering.

Acknowledgments

Funding

Conflicts of interest

The authors declare no conflict of interest.

Authors contribution statement

Conceptualization, R.M., A.E., S.S.H. and M.A.; methodology, A.E., S.S.H., S.H., and A.J.; software, A.E., and S.S.H.; formal analysis, A.E., and S.S.H.; investigation, A.E., S.S.H., S.H., and A.J.; resources, R.M.,; writing—original draft preparation, A.E., S.S.H., S.H., and A.J.; writing—review and editing, R.M., S.S.H., T.-H.K., and Z.W.G.; supervision, R.M., M.A., T.-H.K., Z.W.G. All authors have read and agreed to the published version of the manuscript.

References

[1] Instanes A. Incorporating climate warming scenarios in coastal permafrost engineering design – Case studies from Svalbard and northwest Russia. Cold Reg Sci Technol 2016. https://doi.org/10.1016/j.coldregions.2016.09.004.

[2] Tounsi H, Rouabhi A, Jahangir E, Guérin F. Mechanical behavior of frozen metapelite: Laboratory investigation and constitutive modeling. Cold Reg Sci Technol 2020. https://doi.org/10.1016/j.coldregions.2020.103058.

[3] Zhang J, Fu H, Huang Z, Wu Y, Chen W, Shi Y. Experimental study on the tensile strength and failure characteristics of transversely isotropic rocks after freeze-thaw cycles. Cold Reg Sci Technol 2019. https://doi.org/10.1016/j.coldregions.2019.04.006.

[4]   Foruzanmehr A. Thermal comfort in hot dry climates: Traditional dwellings in Iran. 2017. https://doi.org/10.4324/9781315527130.

[5]   Farajzadeh H, Matzarakis A. Quantification of climate for tourism in the northwest of Iran. Meteorol Appl 2009. https://doi.org/10.1002/met.155.

[6]   Ma Q, Ma D, Yao Z. Influence of freeze-thaw cycles on dynamic compressive strength and energy distribution of soft rock specimen. Cold Reg Sci Technol 2018. https://doi.org/10.1016/j.coldregions.2018.04.014.

[7]   Zhou XP, Li CQ, Zhou LS. The effect of microstructural evolution on the permeability of sandstone under freeze-thaw cycles. Cold Reg Sci Technol 2020. https://doi.org/10.1016/j.coldregions.2020.103119.

[8]   Li J, Kaunda RB, Zhou K. Experimental investigations on the effects of ambient freeze-thaw cycling on dynamic properties and rock pore structure deterioration of sandstone. Cold Reg Sci Technol 2018. https://doi.org/10.1016/j.coldregions.2018.06.015.

[9]   Yang X, Jiang A, Li M. Experimental investigation of the time-dependent behavior of quartz sandstone and quartzite under the combined effects of chemical erosion and freeze–thaw cycles. Cold Reg Sci Technol 2019. https://doi.org/10.1016/j.coldregions.2019.03.008.

[10]   Matsuoka N. Mechanisms of rock breakdown by frost action: An experimental approach. Cold Reg Sci Technol 1990. https://doi.org/10.1016/S0165-232X(05)80005-9.

[11]   Nicholson DT, Nicholson FH. Physical deterioration of sedimentary rocks subjected to experimental freeze-thaw weathering. Earth Surf. Process. Landforms, 2000. https://doi.org/10.1002/1096-9837(200011)25:12<1295::AID-ESP138>3.0.CO;2-E.

[12]   Mutlutürk M, Altindag R, Türk G. A decay function model for the integrity loss of rock when subjected to recurrent cycles of freezing-thawing and heating-cooling. Int J Rock Mech Min Sci 2004. https://doi.org/10.1016/S1365-1609(03)00095-9.

[13]   Altindag R, Alyildiz IS, Onargan T. Mechanical property degradation of ignimbrite subjected to recurrent freeze-thaw cycles. Int J Rock Mech Min Sci 2004. https://doi.org/10.1016/j.ijrmms.2004.03.005.

[14]   Chen TC, Yeung MR, Mori N. Effect of water saturation on deterioration of welded tuff due to freeze-thaw action. Cold Reg Sci Technol 2004. https://doi.org/10.1016/j.coldregions.2003.10.001.

[15]   Karaca Z. Water absorption and dehydration of natural stones versus time. Constr Build Mater 2010. https://doi.org/10.1016/j.conbuildmat.2009.10.029.

[16]   Tan X, Chen Weizhong W, Yang J, Cao J. Laboratory investigations on the mechanical properties degradation of granite under freeze-thaw cycles. Cold Reg Sci Technol 2011. https://doi.org/10.1016/j.coldregions.2011.05.007.

[17]   Bayram F. Predicting mechanical strength loss of natural stones after freeze-thaw in cold regions. Cold Reg Sci Technol 2012. https://doi.org/10.1016/j.coldregions.2012.07.003.

[18]   Gökçe MV, Ince I, Fener M, Taşkiran T, Kayabali K. The effects of freeze-thaw (F-T) cycles on the Gödene travertine used in historical structures in Konya (Turkey). Cold Reg Sci Technol 2016. https://doi.org/10.1016/j.coldregions.2016.04.005.

[19]   Jamshidi A, Nikudel MR, Khamehchiyan M. Predicting the long-term durability of building stones against freeze-thaw using a decay function model. Cold Reg Sci Technol 2013. https://doi.org/10.1016/j.coldregions.2013.03.007.

[20]   Khanlari G, Sahamieh RZ, Abdilor Y. The effect of freeze–thaw cycles on physical and mechanical properties of Upper Red Formation sandstones, central part of Iran. Arab J Geosci 2015. https://doi.org/10.1007/s12517-014-1653-y.

[21]   Bell FG. Engineering properties of soils and rocks. 3rd ed. London: 1993.

[22]   Hori M, Morihiro H. Micromechanical analysis on deterioratIon due to freezing and thawing in porous brittle materials. Int J Eng Sci 1998. https://doi.org/10.1016/S0020-7225(97)00080-3.

[23] Tuğrul A. The effect of weathering on pore geometry and compressive strength of selected rock types from Turkey. Eng Geol 2004. https://doi.org/10.1016/j.enggeo.2004.05.008.

[24] Jamshidi A, Nikudel MR, Khamehchiyan M. A novel physico-mechanical parameter for estimating the mechanical strength of travertines after a freeze–thaw test. Bull Eng Geol Environ 2017. https://doi.org/10.1007/s10064-016-0873-7.

[25] Liping W, Ning L, Jilin Q, Yanzhe T, Shuanhai X. A study on the physical index change and triaxial compression test of intact hard rock subjected to freeze-thaw cycles. Cold Reg Sci Technol 2019. https://doi.org/10.1016/j.coldregions.2019.01.001.

[26] Peng X, Yimin W, Zijian W, Le H. Distribution laws of freeze-thaw cycles and unsaturated concrete experiments in cold-region tunnels. Cold Reg Sci Technol 2020. https://doi.org/10.1016/j.coldregions.2019.102985.

[27] Zhang S, Zhang J, Gui Y, Chen W, Dai Z. Deformation properties of coarse-grained sulfate saline soil under the freeze-thaw-precipitation cycle. Cold Reg Sci Technol 2020. https://doi.org/10.1016/j.coldregions.2020.103121.

[28] Dağdeviren M. Decision making in equipment selection: An integrated approach with AHP and PROMETHEE. J Intell Manuf 2008. https://doi.org/10.1007/s10845-008-0091-7.

[29] Athawale VM, Chakraborty S. Facility Location Selection using PROMETHEE II Method. Int Conf Ind Eng Oper Manag 2010.

[30] Prvulovic S, Dratolmac G, Radovanović LZ. Application of Promethee-Gaia methodology in the choice of systems for drying paltry-seeds and powder materials. Stroj Vestnik/Journal Mech Eng 2011. https://doi.org/10.5545/sv-jme.2008.068.

[31] Bogdanovic D, Nikolic D, Ivana I. Mining method selection by integrated AHP and PROMETHEE method. An Acad Bras Cienc 2012. https://doi.org/10.1590/S0001-37652012005000013.

[32] Abedi M, Ali Torabi S, Norouzi GH, Hamzeh M, Elyasi GR. PROMETHEE II: A knowledge-driven method for copper exploration. Comput Geosci 2012. https://doi.org/10.1016/j.cageo.2011.12.012.

[33] Shirsikar SG, Patil S. Optimization of energy charges using improved PROMETHEE method. ISOR J Commun Eng 2013:36–42.

[34] Balali V, Zahraie B, Roozbahani A. A Comparison of AHP and PROMETHEE Family Decision Making Methods for Selection of Building Structural System. Am J Civ Eng Archit 2014. https://doi.org/10.12691/ajcea-2-5-1.

[35] Mikaeil R, Abdollahi Kamran M, Sadegheslam G, Ataei M. Ranking sawability of dimension stone using PROMETHEE method. J Min Environ (INTERNATIONAL J Min Environ ISSUES) 2015. https://doi.org/10.22044/jme.2015.477.

[36] Mladineo M, Jajac N, Rogulj K. A simplified approach to the PROMETHEE method for priority setting in management of mine action projects. Croat Oper Res Rev 2016. https://doi.org/10.17535/crorr.2016.0017.

[37] Balusa BC, Singam J. Underground Mining Method Selection Using WPM and PROMETHEE. J Inst Eng Ser D 2018. https://doi.org/10.1007/s40033-017-0137-0.

[38] Mikaeil R, Gharahasanlou Jafarnejad E, Aryafar A. Geotechnical Risks Assessment During the Second part of Emamzadeh Hashem (AS) Tunnel Using FDAHP-PROMETHEE. Amirkabir J Civ Eng 2018;49:247–50.

[39] Ghadernejad S, Jafarpour A, Ahmadi P. Application of an integrated decision-making approach based on FDAHP and PROMETHEE for selection of optimal coal seam for mechanization; A case study of the Tazareh coal mine complex, Iran. Int J Min Geo-Engineering 2019. https://doi.org/10.22059/IJMGE.2018.255070.594727.

[40] Iphar M, Alpay S. A mobile application based on multi-criteria decision-making methods for underground mining method selection. Int J Mining, Reclam Environ 2019. https://doi.org/10.1080/17480930.2018.1467655.

[41]   Sitorus F, Cilliers JJ, Brito-Parada PR. Multi-criteria decision making for the choice problem in mining and mineral processing: Applications and trends. Expert Syst Appl 2019. https://doi.org/10.1016/j.eswa.2018.12.001.

[42]   Mikaeil R, Gharahasanlou EJ, Jafarpour A. Ranking and Evaluating the Coal Seam Mechanization Based on Geological Conditions. Geotech Geol Eng 2020. https://doi.org/10.1007/s10706-020-01200-0.

[43]   Dayo-Olupona O, Genc B, Onifade M. Technology adoption in mining: A multi-criteria method to select emerging technology in surface mines. Resour Policy 2020. https://doi.org/10.1016/j.resourpol.2020.101879.

[44]   Dachowski R, Gałek K. Selection of the best method for underpinning foundations using the PROMETHEE II method. Sustain 2020. https://doi.org/10.3390/su12135373.

[45]   Brown ET. Rock characterization testing and monitoring. ISRM suggested methods. Rock Charact Test Monit ISRM Suggest Methods 1981. https://doi.org/10.1016/0148-9062(81)90524-6.

[46]   Naderpour H, Rafiean AH, Fakharian P. Compressive strength prediction of environmentally friendly concrete using artificial neural networks. J Build Eng 2018;16:213–9. https://doi.org/10.1016/j.jobe.2018.01.007.

[47]   Naderpour H, Nagai K, Fakharian P, Haji M. Innovative models for prediction of compressive strength of FRP-confined circular reinforced concrete columns using soft computing methods. Compos Struct 2019;215:69–84. https://doi.org/10.1016/j.compstruct.2019.02.048.

[48]   Dormishi A, Ataei M, Mikaeil R, Khalokakaei R, Haghshenas SS. Evaluation of gang saws' performance in the carbonate rock cutting process using feasibility of intelligent approaches. Eng Sci Technol an Int J 2019;22:990–1000. https://doi.org/10.1016/j.jestch.2019.01.007.

[49]   Shaffiee Haghshenas S, Mikaeil R, Abdollahi Kamran M, Shaffiee Haghshenas S, Hosseinzadeh Gharehgheshlagh H. Selecting the Suitable Tunnel Supporting System Using an Integrated Decision Support System, (Case Study: Dolaei Tunnel of Touyserkan, Iran). J Soft Comput Civ Eng 2019;3:51–66. https://doi.org/10.22115/scce.2020.212995.1150.

[50]   Naderpour H, Rezazadeh Eidgahee D, Fakharian P, Rafiean AH, Kalantari SM. A new proposed approach for moment capacity estimation of ferrocement members using Group Method of Data Handling. Eng Sci Technol an Int J 2020;23:382–91. https://doi.org/10.1016/j.jestch.2019.05.013.

[51]   Ford E, Maneparambil K, Neithalath N. Machine Learning on Microstructural Chemical Maps to Classify Component Phases in Cement Pastes. J Soft Comput Civ Eng 2021;5:1–20. https://doi.org/10.22115/scce.2021.302400.1357.

[52]   Saber A. Effects of Window-to-Wall Ratio on Energy Consumption: Application of Numerical and ANN Approaches. J Soft Comput Civ Eng 2021;5:41–56. https://doi.org/10.22115/scce.2021.281977.1299.

[53]   Shaffiee Haghshenas S, Shaffiee Haghshenas S, Abduelrhman MA, Shervin Z, Mikaeil R. Identifying and Ranking of Mechanized Tunneling Project's Risks by Using A Fuzzy Multi-Criteria Decision Making Technique. J Soft Comput Civ Eng 2022;6:29–45.

[54]   Hosseini SM, Ataei M, Khalokakaei R, Mikaeil R, Haghshenas SS. Investigating the role of coolant and lubricant fluids on the performance of cutting disks (Case study: Hard rocks). Rud Geol Naft Zb 2019. https://doi.org/10.17794/rgn.2019.2.2.

[55]   Mikaeil R, Bakhshinezhad H, Haghshenas SS, Ataei M. STABILITY ANALYSIS OF TUNNEL SUPPORT SYSTEMS USING NUMERICAL AND INTELLIGENT SIMULATIONS (CASE STUDY: KOUHIN TUNNEL OF QAZVIN-RASHT RAILWAY). Rud Zb 2019;34:1–11. https://doi.org/10.17794/rgn.2019.2.1.

[56]   Shirani Faradonbeh R, Shaffiee Haghshenas S, Taheri A, Mikaeil R. Application of self-organizing map and fuzzy c-mean techniques for rockburst clustering in deep underground projects. Neural Comput Appl 2019. https://doi.org/10.1007/s00521-019-04353-z.

[57] Noori AM, Mikaeil R, Mokhtarian M, Haghshenas SS, Foroughi M. Feasibility of Intelligent Models for Prediction of Utilization Factor of TBM. Geotech Geol Eng 2020. https://doi.org/10.1007/s10706-020-01213-9.

[58] Guido G, Haghshenas SS, Haghshenas SS, Vitale A, Gallelli V, Astarita V. Development of a binary classification model to assess safety in transportation systems using GMDH-type neural network algorithm. Sustain 2020. https://doi.org/10.3390/SU12176735.

[59] Morosini AF, Haghshenas SS, Haghshenas SS, Geem ZW. Development of a binary model for evaluating water distribution systems by a pressure driven analysis (PDA) approach. Appl Sci 2020. https://doi.org/10.3390/app10093029.

[60] Kennedy J, Eberhart R. Proceedings of ICNN'95 - International Conference on Neural Networks. Part. Swarm Optim., 1995.

[61] Hasanipanah M, Noorian-Bidgoli M, Jahed Armaghani D, Khamesi H. Feasibility of PSO-ANN model for predicting surface settlement caused by tunneling. Eng Comput 2016. https://doi.org/10.1007/s00366-016-0447-0.

[62] Shahnazar A, Nikafshan Rad H, Hasanipanah M, Tahir MM, Jahed Armaghani D, Ghoroqi M. A new developed approach for the prediction of ground vibration using a hybrid PSO-optimized ANFIS-based model. Environ Earth Sci 2017. https://doi.org/10.1007/s12665-017-6864-6.

[63] Mikaeil R, Shaffiee Haghshenas S, Sedaghati Z. Geotechnical risk evaluation of tunneling projects using optimization techniques (case study: the second part of Emamzade Hashem tunnel). Nat Hazards 2019;97:1099–113. https://doi.org/10.1007/s11069-019-03688-z.

[64] Armaghani DJ, Mohamad ET, Narayanasamy MS, Narita N, Yagiz S. Development of hybrid intelligent models for predicting TBM penetration rate in hard rock condition. Tunn Undergr Sp Technol 2017;63:29–43. https://doi.org/10.1016/j.tust.2016.12.009.

[65] Yagiz S, Ghasemi E, Adoko AC. Prediction of Rock Brittleness Using Genetic Algorithm and Particle Swarm Optimization Techniques. Geotech Geol Eng 2018. https://doi.org/10.1007/s10706-018-0570-3.

[66] Lloyd SP. Least Squares Quantization in PCM. IEEE Trans Inf Theory 1982. https://doi.org/10.1109/TIT.1982.1056489.

[67] Aryafar A, Mikaeil R, Haghshenas SS, Haghshenas SS. Application of metaheuristic algorithms to optimal clustering of sawing machine vibration. Meas J Int Meas Confed 2018. https://doi.org/10.1016/j.measurement.2018.03.056.

[68] Mikaeil R, Haghshenas SS, Hoseinie SH. Rock Penetrability Classification Using Artificial Bee Colony (ABC) Algorithm and Self-Organizing Map. Geotech Geol Eng 2017. https://doi.org/10.1007/s10706-017-0394-6.

[69] Salemi A, Mikaeil R, Haghshenas SS. Integration of Finite Difference Method and Genetic Algorithm to Seismic analysis of Circular Shallow Tunnels (Case Study: Tabriz Urban Railway Tunnels). KSCE J Civ Eng 2018;22:1978–90. https://doi.org/10.1007/s12205-017-2039-y.

[70] Aryafar A, Mikaeil R, Shafiee Haghshenas S. Utilization of soft computing for evaluating the performance of stone sawing machines, Iranian Quarries. Int J Min Geo-Engineering 2018;52:31–6.

[71] Mikaeil R, Beigmohammadi M, Bakhtavar E, Haghshenas SS. Assessment of risks of tunneling project in Iran using artificial bee colony algorithm. SN Appl Sci 2019;1:1711. https://doi.org/10.1007/s42452-019-1749-9.

[72] Guido G, Haghshenas SS, Haghshenas SS, Vitale A, Astarita V, Haghshenas AS. Feasibility of stochastic models for evaluation of potential factors for safety: A case study in southern Italy. Sustain 2020. https://doi.org/10.3390/su12187541.